OCCURRENCE AND STABILITY OF APSIDAL RESONANCE IN MULTIPLE PLANETARY SYSTEMS

Ji-Lin Zhou and Yi-Sui Sun
Department of Astronomy, Nanjing University, Nanjing 210093, China;
zhoujl@nju.edu.cn, sunys@nju.edu.cn

ABSTRACT

With the help of the Laplace-Lagrange solution of the secular perturbation theory in a double-planet system, we study the occurrence and the stability of apsidal secular resonance between the two planets. The explicit criteria for predicting whether two planets are in apsidal resonance is derived, which shows that the occurrence of the apsidal resonance depends only on the mass ratio (m_1/m_2), semimajor axis ratio (a_1/a_2), initial eccentricity ratio (e_{10}/e_{20}), and the initial relative apsidal longitude ($\varpi_{20} - \varpi_{10}$) between the two planets. The probability of two planets falling in apsidal resonance is given in the initial element space. We verify the criteria with numerical integrations for the HD 12661 system and find they give good predictions except at the boundary of the criteria or when the planet eccentricities are too large. The nonlinear stability of the two planets in HD 12661 system are studied by calculating the Lyapunov exponents of their orbits in a general three-body model. We find that two planets in large-eccentricity orbits could be stable only when they are in aligned apsidal resonance. When the planets are migrated under the planet-disk interactions, for more than half of the studied cases, the configurations of the apsidal resonances are preserved. We find the two planets of the HD 12661 system could be in aligned resonance and thus more stable, provided they have $\Omega_2 - \Omega_1 \approx 180°$. The applications of the criteria to the other multiple planetary systems are discussed.

Subject heading: celestial mechanics — methods: analytical — methods: numerical — planetary systems — stars: individual (47 Ursae Majoris, HD 12661)

1. INTRODUCTION

The detection of extrasolar planetary systems has revealed fruitful results during the past years. More than 100 extrasolar planets have been inferred by Doppler radial velocity measurements to the solar-type stars (California and Carnegie Planet Search);[1] among them 10 multiple-planet systems are confirmed. For a multiple-planet system, the dynamical stability of the system under planetary interaction is an important issue concerning the dynamical evolution as well as the possible existence of a habitable zone of the system.

There are many effects that can affect the stability of a multiple-planet system. For the orbits of planets with small or modest eccentricities and inclinations, mean motion resonances between planets can sometimes lead to stable configurations. Another effect is the secular resonance between the planets. An apsidal resonance occurs when the relative apsidal longitudes of the two orbits $\Delta\varpi$ librates about 0 (aligned resonance) and π (antialigned resonance) during the evolution. Because of the aligned apsidal resonance, the two planets on elliptic orbits can greatly reduce the possibility of close encounters; thus, it is believed that aligned apsidal resonance can stabilize the interacting planets.

For the 10 multiple planetary systems observed to date (GJ876, 47 UMa, HD 82943, HD 12661, HD 168443, HD 37124, HD 38529, HD 74156, υ Andromedae, and 55 Cancri), the best-fit orbital parameters inferred from the radial velocity observations show that six pairs of planets could be in apsidal resonance: HD 82943 (Goździewski & Maciejewski 2001), υ Andromedae c and d (Chiang,

Tabachnik, & Tremaine 2001), GJ876 (Lee & Peale 2002), 47 UMa (Laughlin, Chambers, & Fischer 2002), HD 12661 (Goździewski & Maciejewski 2003; Lee & Peale 2003), and 55 Cancri b and c (Ji et al. 2003). Ubiquitous as it is, the apsidal resonance phenomenon is worthy of being studied in detail. In this paper, we are interested in when the apsidal resonance occurs and whether it really leads to a stable configuration between planets, since an antialigned resonance could lead to close encounters between orbits with large eccentricities.

For the occurrence of apsidal resonance, Laughlin et al. (2002) give a criterion based on the Laplace-Lagrange solution of the secular perturbation system. In this paper, the criterion is represented in a more explicit form in § 2. The probability that the apsidal resonance happens is also derived according to the criteria. In § 3, we study the stability of orbits in apsidal resonances by calculating the largest Lyapunov exponents of the orbits with a general three-body model. The behavior of orbits in migration are studied with a torqued three-body model. The conclusions and the applications of the criteria to the other multiple planetary systems are discussed in the final section.

2. LOCATIONS OF APSIDAL RESONANCE

In this section we derive the explicit criteria under which the apsidal secular resonance may occur. To that aim, the linear secular perturbation theory is employed for two interacting planets under the attraction of the host star. For a planetary system with two planets, hereafter we denote all the quantities of the host star, the inner and outer planets with subscripts 0, 1, and 2, respectively. Thus, the three bodies have masses m_0, m_1, and m_2, respectively, where m_1, $m_2 \ll m_0$. In the present study we address the coplanar

---

[1] See the California and Carnegie Planet Search, http://exoplanets.org/planet_table.shtml.

problem only, so the two planets are on the orbits with osculating orbital elements $(a_1, e_1, \varpi_1, M_1)$ and $(a_2, e_2, \varpi_2, M_2)$, respectively, where a, e, ϖ, and M are the semimajor axis, eccentricity, longitude of pericenter, and mean anomaly of the orbit, respectively. We adopt the commonly used unit system, i.e., the mass unit is the solar mass, the length unit is 1 AU, and the time unit is 1 yr$/(2\pi)$.

2.1. Linear Secular Perturbation Theory Revisited

We start with the linear secular theory following Murray & Dermott (1999). For the coplanar case, the disturbing function for the motions of planets m_1 and m_2 are given as

$$R_1 = n_1 a_1^2 \left[\tfrac{1}{2} A_{11} e_1^2 + A_{12} e_1 e_2 \cos(\varpi_1 - \varpi_2)\right],$$
$$R_2 = n_2 a_2^2 \left[\tfrac{1}{2} A_{22} e_2^2 + A_{21} e_1 e_2 \cos(\varpi_1 - \varpi_2)\right], \quad (1)$$

where n_1, and n_2 are the mean motion of planets m_1 and m_2, respectively; A_{ij} are elements of a matrix given by

$$\begin{pmatrix} A_{11} & A_{12} \\ A_{21} & A_{22} \end{pmatrix} = \begin{pmatrix} c_1 & -c_0 c_1 \\ -c_0 c_2 & c_2 \end{pmatrix}, \quad (2)$$

where $c_k > 0$ $(k = 0, 1, 2)$ are functions of a_1, a_2, m_0, m_1, m_2, defined as

$$c_0 = b_{3/2}^{(2)}(\alpha)/b_{3/2}^{(1)}(\alpha) \approx \frac{5}{4}\alpha\left(1 - \frac{1}{8}\alpha^2\right),$$
$$c_1 = \frac{1}{4} n_1 \frac{m_2}{m_0 + m_1} \alpha^2 b_{3/2}^{(1)}(\alpha),$$
$$c_2 = \frac{1}{4} n_2 \frac{m_1}{m_0 + m_2} \alpha b_{3/2}^{(1)}(\alpha), \quad (3)$$

with $b_{3/2}^{(i)}(\alpha)$ $(i = 1, 2)$ being the Laplace coefficients, and $\alpha = a_1/a_2 < 1$. Figure 1 shows the approximation of c_0 by the above formula. Quantitatively, the error of approximation is less than 1% for $\alpha < 0.66$ and less than 5% for $\alpha < 0.91$. So the approximation is quite good for the study of the planetary system. Moreover, we define

$$\xi = \frac{c_2}{c_1} = \frac{1}{\alpha}\frac{n_2 m_1 (m_0 + m_1)}{n_1 m_2 (m_0 + m_2)} \approx q\alpha^{1/2}, \quad (4)$$
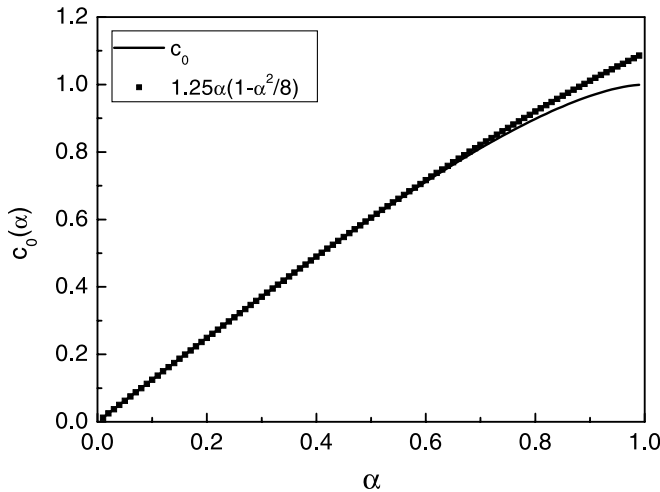
with $q = m_1/m_2$, and the terms with orders of

$O(m_1/m_0)$, $O(m_2/m_0)$ or higher are neglected in the above approximation, since m_1/m_0, $m_2/m_0 \sim 10^{-3}$ in the planetary systems. Denote g_1, g_2 as the two eigenvalues of matrix (2), and the corresponding eigenvectors are

$$S_i \begin{pmatrix} \cos\theta_i \\ \sin\theta_i \end{pmatrix},$$

where $\theta_i \in (-\pi/2, \pi/2)$ and

$$\cos\theta_i = \frac{c_0 c_1}{\sqrt{(c_1 - g_i)^2 + c_0^2 c_1^2}},$$
$$\sin\theta_i = \frac{c_1 - g_i}{\sqrt{(c_1 - g_i)^2 + c_0^2 c_1^2}}, \quad i = 1, 2, \quad (5)$$

with

$$g_1 = \tfrac{1}{2}\left[(c_1 + c_2) + \sqrt{(c_1 - c_2)^2 + 4c_0^2 c_1 c_2}\right],$$
$$g_2 = \tfrac{1}{2}\left[(c_1 + c_2) - \sqrt{(c_1 - c_2)^2 + 4c_0^2 c_1 c_2}\right]. \quad (6)$$

Define

$$\rho_1 \equiv \tan\theta_1 = \frac{1}{2c_0}\left[1 - \xi - \sqrt{(1 - \xi)^2 + 4c_0^2\xi}\right],$$
$$\rho_2 \equiv \tan\theta_2 = \frac{1}{2c_0}\left[1 - \xi + \sqrt{(1 - \xi)^2 + 4c_0^2\xi}\right]. \quad (7)$$

So $\rho_1 < 0$ and $\rho_2 > 0$, or $-\pi/2 < \theta_1 < 0 < \theta_2 < \pi/2$. The scaling factor S_i $(i = 1, 2)$ can be expressed in terms of initial eccentricities e_{10}, e_{20} and $\Delta\varpi_0 = \varpi_{20} - \varpi_{10}$,

$$S_1 = \frac{(\rho_2^2 e_{10}^2 - 2\rho_2 e_{10} e_{20} \cos\Delta\varpi_0 + e_{20}^2)^{1/2}}{|\rho_1 - \rho_2|\cos\theta_1}$$
$$\equiv \frac{F}{|\rho_1 - \rho_2|\cos\theta_1},$$
$$S_2 = \frac{(\rho_1^2 e_{10}^2 - 2\rho_1 e_{10} e_{20} \cos\Delta\varpi_0 + e_{20}^2)^{1/2}}{|\rho_1 - \rho_2|\cos\theta_2}$$
$$\equiv \frac{G}{|\rho_1 - \rho_2|\cos\theta_2}. \quad (8)$$

The secular system with disturbing functions (1) is integrable and the solutions can be written as

$$e_1 = \frac{1}{|\rho_1 - \rho_2|}\left(F^2 + 2FG\cos\Delta\psi + G^2\right)^{1/2},$$
$$e_2 = \frac{1}{|\rho_1 - \rho_2|}$$
$$\times \left(\rho_1^2 F^2 + 2\rho_1\rho_2 FG\cos\Delta\psi + \rho_2^2 G^2\right)^{1/2},$$
$$e_1 e_2 \sin\Delta\varpi = -\frac{1}{\rho_1 - \rho_2} FG\sin\Delta\psi,$$
$$e_1 e_2 \cos\Delta\varpi = \frac{1}{(\rho_1 - \rho_2)^2}$$
$$\times \left[\rho_1 F^2 + (\rho_1 + \rho_2)FG\cos\Delta\psi + \rho_2 G^2\right], \quad (9)$$

where $\Delta\psi = \psi_2 - \psi_1 = (g_2 t + \beta_2) - (g_1 t + \beta_1)$, with t the

time and β_1, β_2 given by

$$\sin \beta_1 = \frac{1}{F}(h_{10}\rho_2 - h_{20}), \quad \sin \beta_2 = -\frac{1}{G}(h_{10}\rho_1 - h_{20}),$$

$$\cos \beta_1 = \frac{1}{F}(k_{10}\rho_2 - k_{20}), \quad \cos \beta_2 = -\frac{1}{G}(k_{10}\rho_1 - k_{20}),$$

$$(10)$$

where $h_{i0} = e_{i0} \sin \varpi_{i0}$, $k_{i0} = e_{i0} \cos \varpi_{i0}$, $(i = 1, 2)$. From equation (9), it is easy to verify that the evolution of e_1, e_2 obeys an integral,

$$\frac{e_1^2}{A_{12}} + \frac{e_2^2}{A_{21}} = D, \qquad (11)$$

where D is a constant that depends only on the initial parameters. Moreover, from equations (8) and (9), the maximum of e_1 and minimum of e_2 occur at $\cos \Delta \psi = 1$ (as $\rho_1 < 0$), with values

$$e_{1\,max} = \frac{F + G}{|\rho_1 - \rho_2|}, \quad e_{2\,min} = \frac{|\rho_1 F + \rho_2 G|}{|\rho_1 - \rho_2|}. \qquad (12)$$

The minimum of e_1 and maximum of e_2 occur at $\cos \Delta \psi = -1$, with

$$e_{1\,min} = \frac{|F - G|}{|\rho_1 - \rho_2|}, \quad e_{2\,max} = \frac{\rho_2 G - \rho_1 F}{|\rho_1 - \rho_2|}. \qquad (13)$$

Thus, we can obtain the maximum excursions of e_1 and e_2 for any given $e_{10}, e_{20}, \Delta \varpi_0$ as follows:

$$\Delta e_1 = \frac{(F + G) - |F - G|}{|\rho_1 - \rho_2|},$$

$$\Delta e_2 = \frac{(\rho_2 G - \rho_1 F) - |\rho_1 F + \rho_2 G|}{|\rho_1 - \rho_2|}. \qquad (14)$$

2.2. The Explicit Criteria

With the help of the last equation of (9), the criterion in Laughlin et al. (2002) for the apsidal resonance can be expressed as

$$S = \left| \frac{(\rho_1 + \rho_2)FG}{\rho_1 F^2 + \rho_2 G^2} \right| < 1. \qquad (15)$$

Since when $S < 1$, the values of $\Delta \varpi$ cannot reach $\pi/2$ or $3\pi/2$ (thus, $\cos \Delta \varpi \neq 0$), it must librate about 0 or π. On the contrary, when $S > 1$, it is possible that $\Delta \varpi$ will reach $\pi/2$ or $3\pi/2$; thus, it will circulate in $[0, 2\pi]$.

Equation (15) is equivalent to, after some algebra manipulations,

$$\frac{F}{G} > \max\left(1, -\frac{\rho_1}{\rho_2}\right), \quad \text{or} \quad 0 < \frac{F}{G} < \min\left(1, -\frac{\rho_1}{\rho_2}\right), \quad (16)$$

In view of equation (8), the above relations are equivalent to

$$\frac{e_{20}}{e_{10}} < \frac{2\rho_1\rho_2}{\rho_1 + \rho_2} \cos \Delta \varpi_0, \qquad (17)$$

or

$$\frac{e_{20}}{e_{10}} > \frac{\rho_1 + \rho_2}{2} \frac{1}{\cos \Delta \varpi_0} > 0. \qquad (18)$$

By substituting equations (3), (4), and (7) into the above expressions, we finally obtain

$$\frac{e_{20}}{e_{10}} < -\frac{5}{2} \frac{q\alpha^{3/2}[1 - (1/8)\alpha^2]}{1 - q\alpha^{1/2}} \cos \Delta \varpi_0, \qquad (19)$$

or,

$$\frac{e_{20}}{e_{10}} > \frac{2}{5} \frac{1 - q\alpha^{1/2}}{\alpha[1 - (1/8)\alpha^2]} \frac{1}{\cos \Delta \varpi_0} > 0. \qquad (20)$$

These are the explicit criteria for the occurrence of the apsidal secular resonance. Equations (17) and (18) are obtained with the linear secular perturbation theory, while to get equations (19) and (20), we use the approximations of c_0 and ξ in equations (3) and (4).

We call the libration region defined in equation (19) the down-libration region and that defined in equation (20) the up-libration region. Whether the down-libration or up-libration is the aligned or antialigned resonance depends on the sign of $(1 - q\alpha^{1/2})$. For $q\alpha^{1/2} < 1$, down-libration occurs only when $\pi/2 < \Delta \varpi_0 < 3\pi/2$ (thus, it is the antialigned resonance) and up-libration occurs when $\Delta \varpi_0 < \pi/2$, $\Delta \varpi_0 > 3\pi/2$ (the aligned resonance). This is the case in the HD 12661 system. If $q\alpha^{1/2} > 1$, the conclusions are reversed, which is the case in the 47 UMa system. For the critical case $q\alpha^{1/2} = 1$, according to equations (19) and (20), all the orbits are in libration except those with $\Delta \varpi_0 = \pi/2, 3\pi/2$. Figure 2 shows a typical phase space and the evolution of an orbit in the linear secular perturbation system (1). The jumps of $\Delta \varpi$ are due to the crossing of the origin in the $(e_i \cos \varpi_i, e_i \sin \varpi_i)$ plane. Figure 3 shows the resonance region in the e_{20}-$\Delta \varpi_0$ plane defined by equations (19) and (20) with different e_{10}. The parameters α and q are taken from the planetary systems HD 12661 and 47 UMa (listed in Tables 1 and 2). The boxes around the present configuration dots show the uncertainties of the elements (also listed in Tables 1–2).

There are two limiting cases for criteria (19) and (20):

1. $\alpha \to 0$.—The minimum e_{20} for up-libration and maximum e_{20} for down-libration can be obtained by setting $\cos \Delta \varpi = 1$ in equations (19) and (20). When $\alpha \to 0$, the minimum e_{20} for up-libration tends to very large and maximum e_{20} for down-libration tends to zero. So when the two planets are far away, the libration regions in the e_{20}-$\Delta \varpi_0$ plane can be negligibly small.

2. $e_{i0} \to 0$.—This happens when one of the planets is in a nearly circular orbit, and it is just the case discussed in Malhotra (2002), namely, for two planets initially in nearly circular orbits, an impulse perturbation may impart a finite eccentricity to one planet's orbit.

When $e_{10} \to 0$, criterion (20) is always fulfilled if $-\pi/2 < \Delta \varpi_0 < \pi/2$ for $q\alpha^{1/2} < 1$ or $\pi/2 < \Delta \varpi_0 < 3\pi/2$ for $q\alpha^{1/2} > 1$. The boundary curves are the limits of those with e_{10} tending to zero in Figure 3a or 3b, with both the minimum e_{20} for up-libration and the maximum e_{20} for down-libration tending to zero. Thus, half of the e_{20}-$\Delta \varpi_0$ plane is the possible resonance region with up-libration. Thus, the probability of these two planets captured into apsidal resonance tends to 50%. This conclusion agrees with that of Malhotra (2002). It is possible that these two planets are captured in antialigned apsidal resonance, which depends on the sign of $1 - q\alpha^{1/2}$. Similarly, when $e_{20} \to 0$, criterion
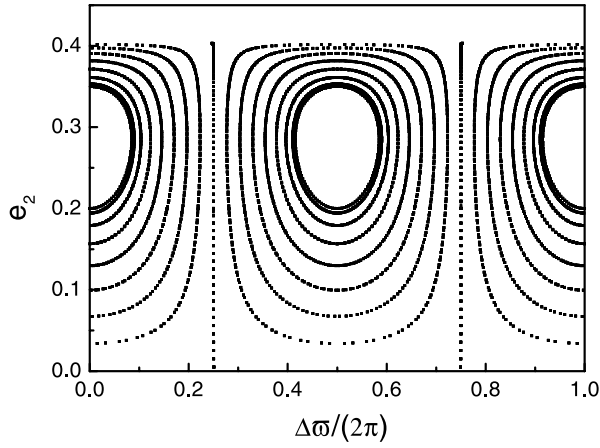
FIG. 2a
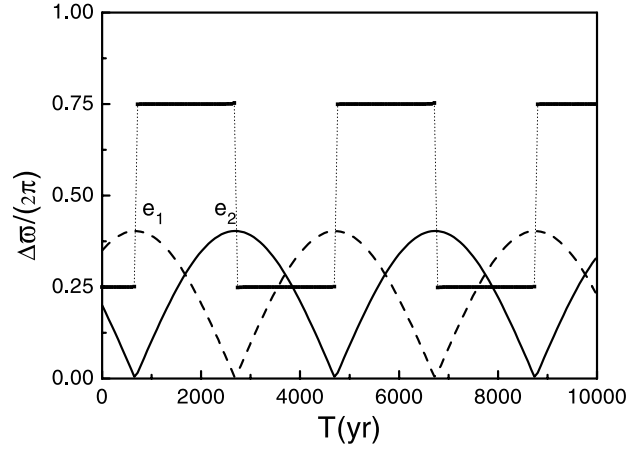

FIG. 2b

FIG. 2.—Critical case of HD 12661 with the observed a_1 and q but with $a_2 = a_1 q^2 \approx 1.76$ AU. (a) The phase plane e_2-$\Delta\varpi$; the orbits in the diagram have the same constant D as that of $e_{10} = 0.35$, $e_{20} = 0.20$. (b) Variation of e_1, e_2, $\Delta\varpi$ with time for an orbit with $\Delta\varpi_0 = \pi/2$.

(19) is always fulfilled; thus, half of the e_{20}-$\Delta\varpi_0$ plane is a possible resonance region with down-libration, and the probability of the two planets being in apsidal resonance (either aligned or antialigned resonance) tends to 50%.

To compare the above libration regions obtained by the criteria with those calculated from the secular perturbation system, we integrate the orbits of the secular perturbation system for the HD 12661 system. Figure 4 shows the diagrams of orbits in e_2-$\Delta\varpi$ plane; the initial values of the studied orbits have $e_{10} = 0.1$, with $\Delta\varpi_0 = 0$ for Figure 3a and $\Delta\varpi_0 = \pi$ for Figure 3b. According to criteria (19) and (20), $e_{20} > 0.022$ for the aligned resonance at $\Delta\varpi_0 = 0$, and $e_{20} < 0.375$ for the antialigned resonance at $\Delta\varpi_0 = \pi$, which coincide with the values given from the secular perturbation system.

Figure 5 shows the contours of the excursions of e_1, e_2 for different e_{20} and $\Delta\varpi_0$. As we can see, generally the orbits in apsidal resonance have relatively smaller Δe_1, Δe_2, especially the turning points of the contour curves lie in one of the libration boundary curves. Thus from the linear secular perturbation theory, the orbits in apsi-

dal resonance, either in aligned resonance or antialigned resonance, are more stable than those in nonresonance regions.

2.3. Area of the Libration Region

From the above criteria, we can calculate the probability that the two planets fall in apsidal resonance in the space of initial orbital elements . We define the probability as the area of the libration region in the e_{20}-$\Delta\varpi_0$ plane for a given e_{10}. For the down-libration case, according to equation (19), it is possible that the peak value of the e_{20}-$\Delta\varpi_0$ curve can be above unit for larger e_{10} (as the $e_{10} = 0.35$ case in Fig. 3a, and the $e_{10} = 0.50$ case in Fig. 3b). We set $\Delta\varpi_d$ as the half-width of the down-libration region where the boundary curve reaches $e_{20} = 1$. Figures 3a and 3b show $\Delta\varpi_d$ for the $e_{10} = 0.35$ and $e_{10} = 0.50$ curves, respectively. Define

$$Q_d = \frac{5}{2} \frac{e_{10} q \alpha^{3/2}[1 - (1/8)\alpha^2]}{|1 - q\alpha^{1/2}|} ; \qquad (21)$$
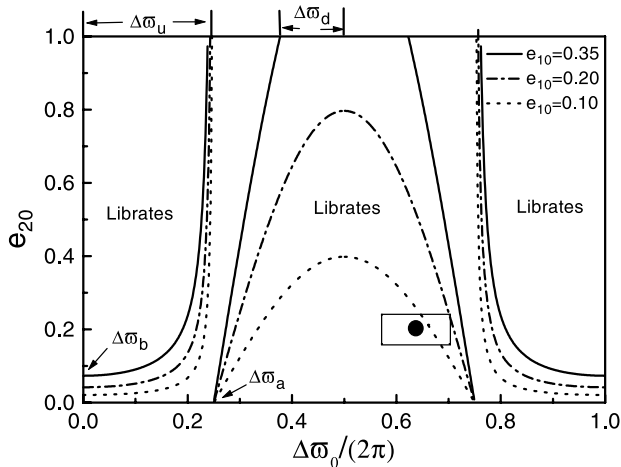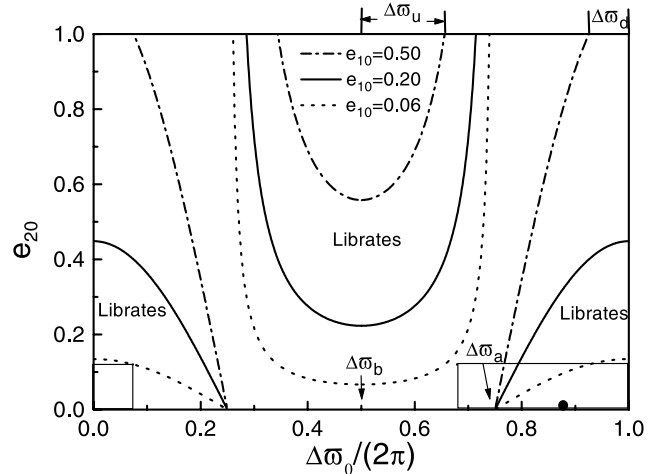

FIG. 3a

FIG. 3b

FIG. 3.—Libration region in the e_{20}-$\Delta\varpi_0$ plane defined by eqs. (19) and (20) with different e_{10} for α and q equal to (a) the planetary system HD 12661 and (b) 47 Uma. The black dots show the present configuration of the two planets in both systems, around which the boxes show the uncertainties of the orbital elements in Tables 1 and 2. The values $\Delta\varpi_a$, $\Delta\varpi_b$ are the lower integration limits in eqs. (23) and (26), respectively, and $\Delta\varpi_d$, $\Delta\varpi_u$ are defined in eqs. (22) and (25), respectively.

TABLE 1
ORBITAL PARAMETERS[a] FOR HD 12661(1.07 $M_\odot$) SYSTEM

Parameter	HD 12661 b	HD 12661 c
Planet mass $M\sin i$ (M_{Jup}).......	2.30	1.57
Period P (days).....................	263.6 (1.2)	1444.5 (12.5)
T_p (JD) (days)	2,449,941.9 (6.2)	2,449,733.6 (49.0)
Semimajor axis a (AU)...........	0.82	2.56
Eccentricity e	0.35 (0.03)	0.20 (0.04)
Argument of pericenter ω (deg)	293.1 (5.0)	162.4 (18.5)

[a] Data from Fischer et al. 2003.

TABLE 2
ORBITAL PARAMETERS[a] FOR 47 UMa (1.03 $M_\odot$) SYSTEM

Parameter	47 UMa b	47 UMa c
Planet mass $M\sin i$ (M_{Jup})...	2.54	0.76
Period P (days)...................	1089.0 (2.9)	2594 (90)
T_p (JD) (days)	2,450,356.0 (33.6)	2,451,363.5 (495.3)
Semimajor axis a (AU).......	2.09	3.73
Eccentricity e	0.061 (0.014)	0.005 (0.115)
Argument of pericenter ω (deg)	171.8 (15.2)	127.0 (55.8)

[a] Data from Fischer et al. 2002.

then

$$\Delta\varpi_d = \begin{cases} \arccos(1/Q_d), & \text{if } Q_d > 1 \\ 0, & \text{if } Q_d \leq 1 \end{cases}, \quad (22)$$

and the area ratio of the down-libration area to the total area of e_{20}-$\Delta\varpi_0$ plane is

$$P_d = \frac{1}{\pi}\left(\Delta\varpi_d + \int_{\Delta\varpi_a}^{\Delta\varpi_a+\pi/2-\Delta\varpi_d} Q_d \cos\Delta\varpi \, d\Delta\varpi\right)$$

$$= \frac{1}{\pi}[\Delta\varpi_d + Q_d(1 - \sin\Delta\varpi_d)], \quad (23)$$

where the lower integration limit is the beginning point of the down-libration region in the $\Delta\varpi_0$-axis ($\Delta\varpi_a = \pi/2$ for $q\alpha^{1/2} < 1$ and $\Delta\varpi_a = 3\pi/2$ for $q\alpha^{1/2} > 1$). Figures 3a and 3b show the $\Delta\varpi_a$ for the $e_{10} = 0.35$ and $e_{10} = 0.50$ curves, respectively. As one can see, the area ratio for the down-libration increases linearly with e_{10} when e_{10} is small, since in the interval one has $\Delta\varpi_d = 0$ in equation (23). However, for larger e_{10}, the increase of area ratio is no longer linear since $\Delta\varpi_d \neq 0$.

Similarly, for the up-libration resonance, if we set $\Delta\varpi_u$ as the half-width of the up-libration region when the boundary

curve meets $e_{20} = 1$ (see Fig. 3) and define

$$Q_u = \frac{2}{5}\frac{e_{10}|1 - q\alpha^{1/2}|}{\alpha[1 - (1/8)\alpha^2]}, \quad (24)$$

we see

$$\Delta\varpi_u = \arccos(Q_u), \quad (25)$$

and the area ratio of the up-libration area to the total area of e_{20}-$\Delta\varpi_0$ plane is

$$P_u = \frac{1}{\pi}\left(\Delta\varpi_u - \int_{\Delta\varpi_b}^{\Delta\varpi_b+\Delta\varpi_u} Q_u \frac{1}{\cos\Delta\varpi} d\Delta\varpi\right)$$

$$= \frac{1}{\pi}\left[\Delta\varpi_u - Q_u \ln\left(\frac{1 + \sin\Delta\varpi_u}{\cos\Delta\varpi_u}\right)\right], \quad (26)$$

where the lower integration limit $\Delta\varpi_b$ is the center of the up-libration region ($\Delta\varpi_b = 0$ for $q\alpha^{1/2} < 1$ and $\Delta\varpi_b = \pi$ for $q\alpha^{1/2} > 1$; see Fig. 3).

In the early evolution of planetary systems, both q and α may vary because of planetary formation and migration. We fix $e_{10} = 0.35$ for the HD 12661 systems and see the variation of libration area ratio with α or q. Figure 6 shows the variation of libration area ratios with α and q. In Figure 6a,
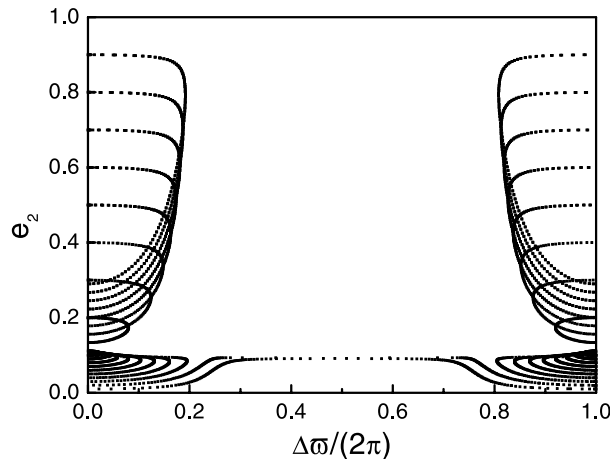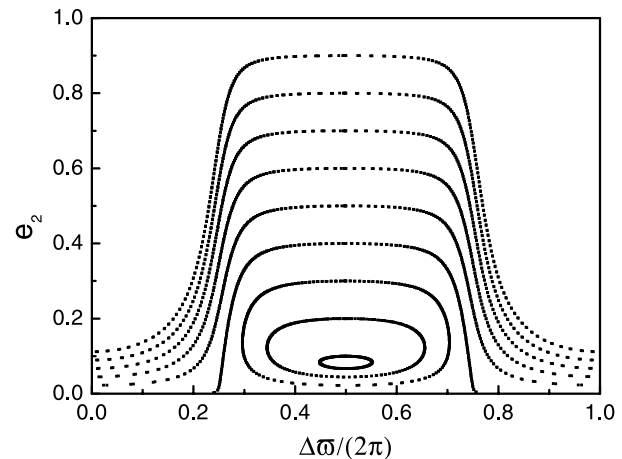

FIG. 4a

FIG. 4b

FIG. 4.—Orbital diagrams of planet system HD 12661 with initial values (a) $e_{10} = 0.1$, $\Delta\varpi_0 = 0$ and (b) $e_{10} = 0.1$, $\Delta\varpi_0 = \pi$
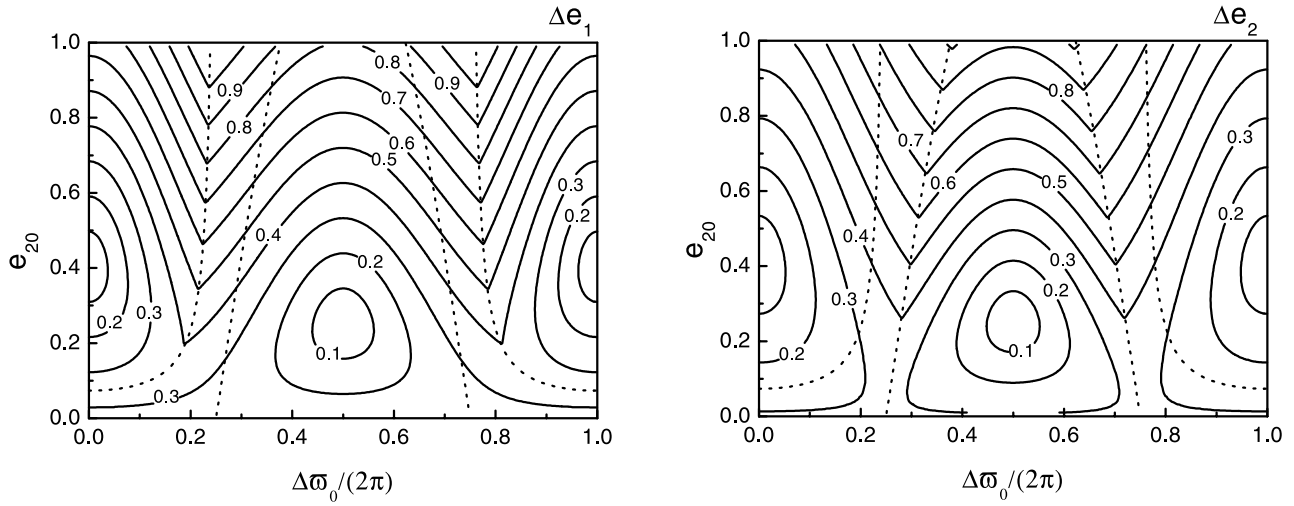
FIG. 5.—Contours of Δe_1, Δe_2 defined by eq. (14) in the initial e_{20}-$\Delta \varpi_0$ plane with $e_{10} = 0.35$. The dotted lines are the boundary of the libration region defined in eqs. (19) and (20).

$q \approx 1.46$ is fixed as the observed value. One can see the ratios increase with α before they reach the maximum (unit) at $\alpha_{max} = q^{-2} \approx 0.47$, which is the critical case, and then decrease. In Figure 6b, $\alpha \approx 0.32$ is fixed as the observed values. Again the curves reach the maximum at $q = \alpha^{-1/2} \approx 1.76$, the critical case.

3. STABILITY OR ORBITS IN RESONANCE

Since the linear secular perturbation theory is an approximation to the real three-body system, the above criteria obtained from the linear perturbation theory has its limitation. To apply the linear criteria to the predicting of the apsidal secular resonance, we integrate the orbits in a general three-body (coplanar) system, where the longitudes of the ascending nodes and the inclinations of the two planet orbits are assumed to be zero ($\Omega_1 = \Omega_2 = 0$, $i_1 = i_2 = 0$) in the paper. We adopt the Runge-Kutta-Fehlberg integrator RKF7(8) with adaptive step sizes to integrate the orbits. Generally the step is alternated between 0.00625 and 0.0125

yr, so there are 80–160 steps in a period of planet orbit with a semimajor axis of 1 AU, and the final error of the Hamiltonian of the three-body system after 10 Myr evolution is less than 10^{-9}.

We define an index to indicate whether an orbit is in libration region or not. We choose a serial of discrete time during the evolution of orbits (for example, every 12.5 yr) and give an index I_n for each time, so that $I_n = 0$ if at that time $-\pi/2 < \Delta \varpi < \pi/2$, and $I_n = 1$ if $\pi/2 < \Delta \varpi < 3\pi/2$. Then the average values of I_n over very large n, denoted by $\langle I_n \rangle$, shows roughly the character of the orbit during the studied period of time according to

$$\text{Index} = \langle I_n \rangle \approx \begin{cases} 0 & \text{aligned libration} \\ 0.5 & \text{circulation} \\ 1 & \text{antialigned libration} \\ \text{others} & \text{mixed} \end{cases}. \quad (27)$$

Figure 7 shows the index for the HD 12661 planet system for 10×51 orbits in the interval $[0, 0.5] \times [0, \pi]$ of the
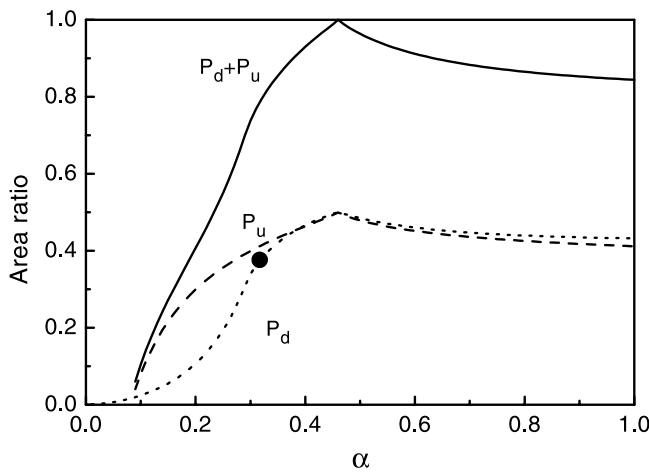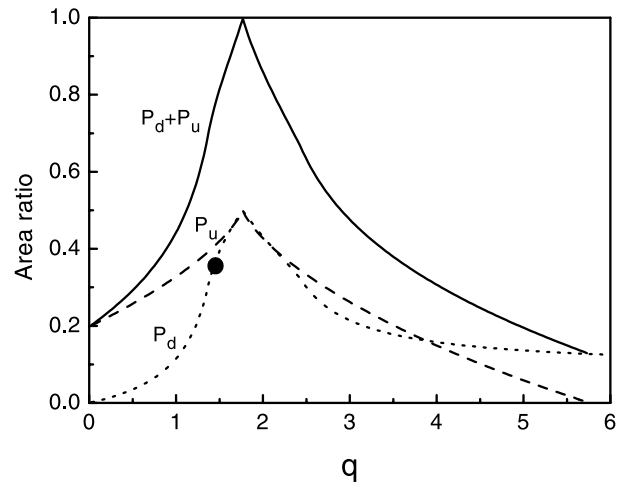

FIG. 6a

FIG. 6b

FIG. 6.—Variations of the libration area ratios with α and q for the planet system HD 12661. (a) The observed $q \approx 1.46$ is fixed, and (b) the observed $\alpha \approx 0.32$ fixed. In both diagrams $e_{10} = 0.35$ is fixed. The black dot in each plot shows the location of observed configuration.
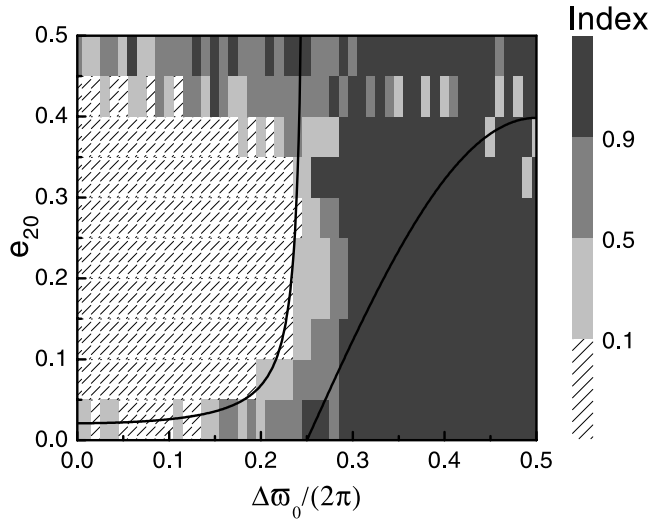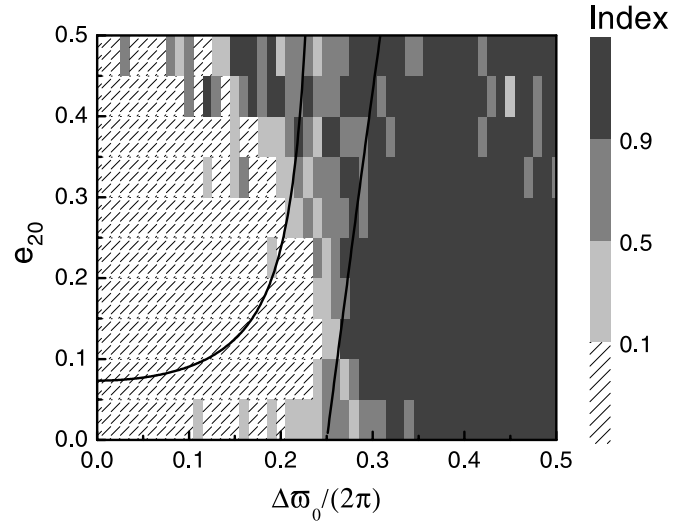
FIG. 7a

FIG. 7b

FIG. 7.—Libration regions in the e_{20}-$\Delta\varpi_0$ plane in the general three-body system for the HD 12661 system. The solid curves show the boundary defined in eqs. (19) and (20). The initial eccentricity is (a) $e_{10} = 0.10$ and (b) $e_{10} = 0.35$.

e_{20}-$\Delta\varpi_0$ plane (the same for the following calculations), the initial eccentricity is $e_{10} = 0.10$ in Figure 7a and $e_{10} = 0.35$ in Figure 7b. As one can see, most of the orbits in the libration region predicted by linear criteria (19) and (20) are in the real libration region when e_{20} is small. The discrepancies between the linear system and the three-body one mainly occur for larger values of e_{20} and the boundary between the libration and circulation region.

Next we want to see whether the orbits, either in apsidal resonance or not, have different stability in the general coplanar three-body model. The stability of an orbit in a Hamiltonian system is related with the topology (regular or chaotic) of the phase space, so we calculate the largest Lyapunov characteristic exponent (LCE) to indicate whether the corresponding orbit is in a regular or chaotic region. The LCE at finite time $\chi(t)$ is calculated for few orbits up to $t = 10$ Myr (denoted as χ_7), and for most orbits up to $t = 1$ Myr (denoted by χ_6). Figure 8 shows the LCEs
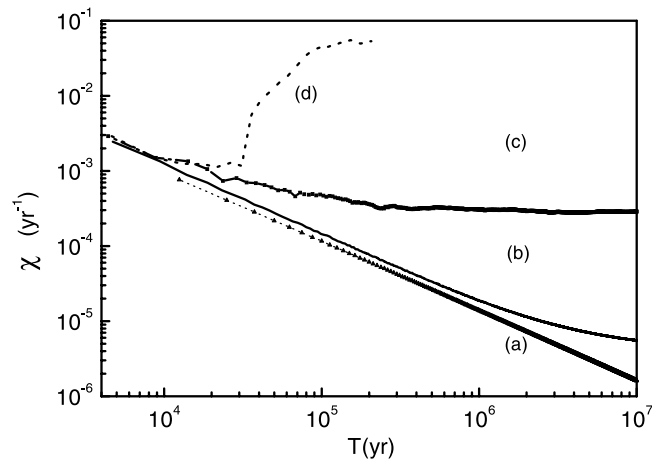

FIG. 8.—LCE $\chi(t)$ for (curve a) the 47 UMa system with the observed orbital parameters listed in Table 2; curve b: the HD 12661 system with the observed orbital parameters listed in Table 1; curve c: same parameters as in curve b, except $e_{20} = 0.20$, $\varpi_{10} = 0$, and $\varpi_{20} = 0.6\pi$; curve d: same parameters as in curve b, except $e_{20} = 0.35$, $\varpi_{10} = 0$, $\varpi_{20} = 0.7\pi$; the outer planet escapes at time $t \approx 2.1 \times 10^5$ yr.

of four orbits in the four different kinds of region in the phase space. For curve a, $\chi(t)$ decrease linearly with t; thus, the orbit corresponding to curve a has zero LCE and is in a regular region. Curve b shows a very small but nonzero LCE, so the orbit corresponding to curve b is in a very weak chaotic region. Both curves a and b have $\chi_6 \sim 10^{-5}$ yr^{-1}, $\chi_7 \sim 10^{-6}$ yr^{-1}. Curve c tends to a constant value, with $\chi_6 \approx \chi_7 \sim 10^{-4}$ yr^{-1}, so the orbit corresponding to curve c should be in a strong chaotic region. The orbit corresponding to curve d is unstable with the outer planet escape before 10^7 Myr, and $\chi(t)$ for such an orbit is generally great than 10^{-2} yr^{-1} before escape. Thus, by calculating χ_6 (in units of yr^{-1}), we can identify at least three different kinds of orbits:

$$\chi_6 \in \begin{cases} (10^{-5}, 10^{-4}] & \text{regular or weak chaos} \\ (10^{-4}, 10^{-2}] & \text{strong chaos} \\ (10^{-2}, 10^{-1}] & \text{unstable} \end{cases} \quad . \quad (28)$$

We calculate χ_6 for the HD 12661 system with initial eccentricity $e_{10} = 0.10$ in one run and $e_{10} = 0.35$ in another run, and the other initial parameters are taken as the observed values. Figure 9 shows the results. The boundary curves for the corresponding e_{10} are also plotted in the diagram. We find for small e_{10} that the orbits, whether in aligned resonance, antialigned resonance, or nonresonance regions, do not show much difference about the LCEs. Thus, in this case, whether or not an orbit is in apsidal resonance does not strongly affect its stability. However, for larger initial e_{10}, orbits in aligned resonance seem to be more, stable since they have much lower LCE as compared with those in the antialigned resonance or circulation regions with same e_{20}. This example shows that for larger e_{10} and e_{20}, planets in aligned resonance regions would be relatively more stable. From Figure 9b, we can also see the present configuration of HD 12661b and HD 12661c is in the boundary of a chaotic region, if $\Delta\varpi_0$ is set to $130^\circ.7$, which is symmetric with the observed value of $-130^\circ.7$. This conclusion has been obtained by Kiseleva-Eggleton et al. (2002).

Finally, we study the role of apsidal resonance on the stability of the orbits when the planets are migrating. In the
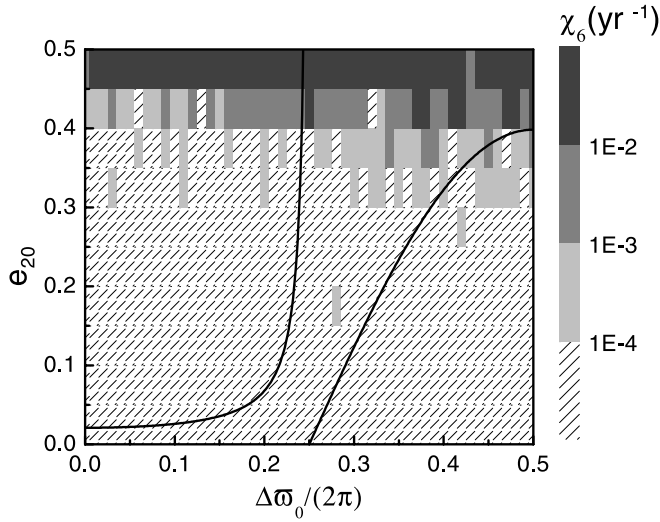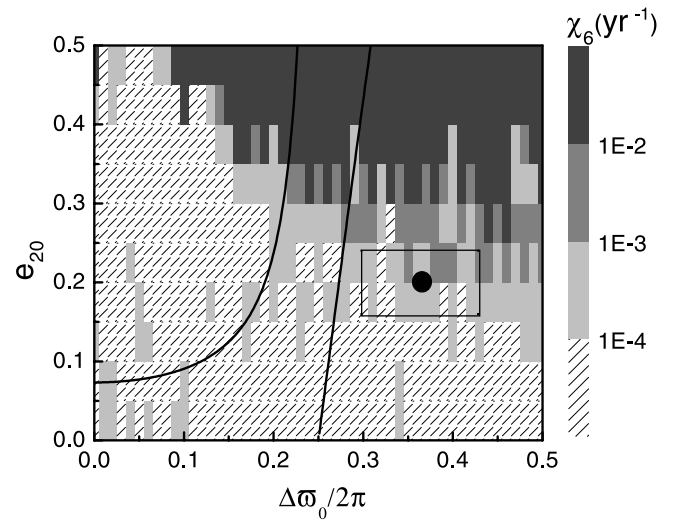
FIG. 9a

FIG. 9b

FIG. 9.—LCE χ_6 for the HD 12661 system. The initial eccentricity is (a) $e_{10} = 0.10$, (b) $e_{10} = 0.35$. The solid curves show the boundary defined in eqs. (19) and (20). The black dot in (b) shows the location of observed configuration with $\Delta\varpi_0 = 130°7$, around which the box shows the uncertainties of the orbital elements.

early stage of planet evolution, the protoplanets and the stellar disk might be coexisting and interacting; thus, planet migration might happen because of nebular tides (see, e.g., Ward 1997). We adopt the torqued three-body model as in Laughlin et al. (2002), and for the sake of simplicity we consider the case in which only the outer planet experiences an azimuthal torque due to the planet-disk interaction. We take the azimuthal acceleration as $f_2 = -2 \times 10^{-6}$ AU^2 yr^{-1} (which is smaller than that used in Laughlin et al. 2002, because here we are concerned with the qualitative evolutions only) and study both the forward ($t > 0$) and backward ($t < 0$) evolutions of orbits under this acceleration. We calculate the orbits for the HD 12661 system with initial $e_{10} = 0.35$, and M_{10}, M_{20} are randomly chosen. All the other initial parameters of orbits are taken from Table 1. The evolution time span is 50,000 yr. In concurrence with Laughlin et al. (2002), we find that in all the studies cases (both for-

ward and backward), the semimajor axis of the inner planet does not have secular changes. Figure 10a shows the index for the orbits during the evolution, and Figure 10b shows the a_2 at the final time for the forward case. Some of the orbits that were initially in apsidal resonance region become mixed, although, according to Figure 6a, the libration regions are enlarged because of the increase of α (from 0.32 to approximately 0.41) by planet migration. For orbits in the aligned resonance, they are more stable and have smaller final a_2, while for orbits in antialigned resonance with larger e_{20}, or in circulation region, they tend to be more unstable because of close encounters and thus have larger final a_2, and most of them will escape soon in the following evolutions. Figure 11 shows the backward case. We find the conclusions are more or less similar. Although the libration regions shrink because of the decrease of α by the planet migration (from 0.32 to approximately 0.23) in this case, the
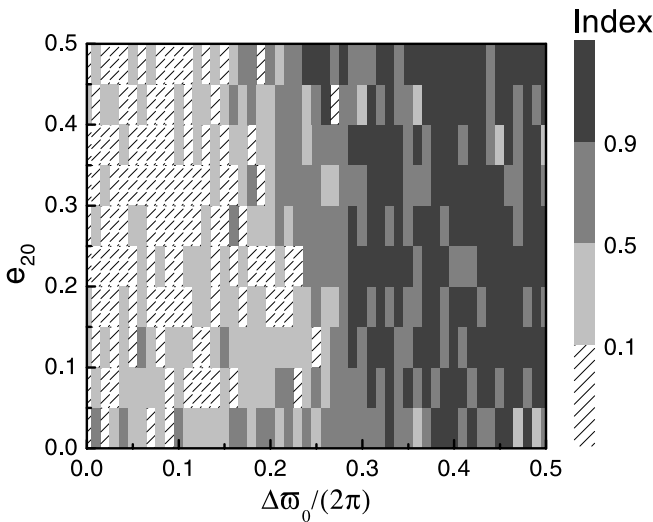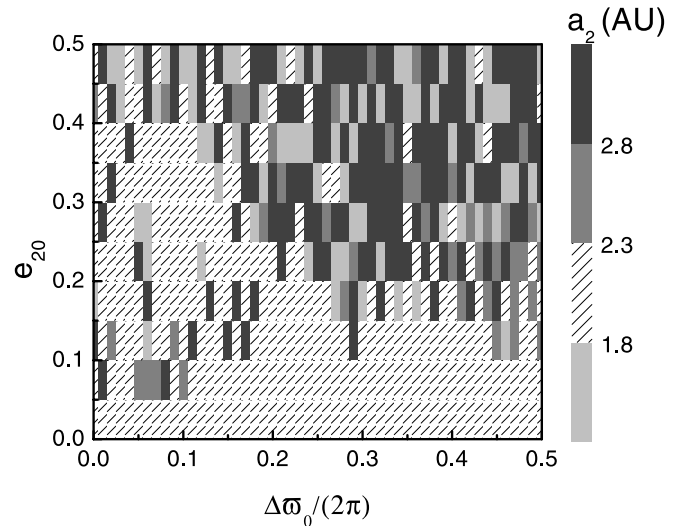

FIG. 10a

FIG. 10b

FIG. 10.—(a) Index of libration region and (b) the relative semimajor axis of the two planets in the HD 12661 system under azimuthal acceleration $f_2 = -2 \times 10^{-6}$ AU^2 yr^{-1}. The initial eccentricity is $e_{10} = 0.35$ and M_{10}, M_{20} are randomly chosen. The time evolution is $t = 50,000$ yr.
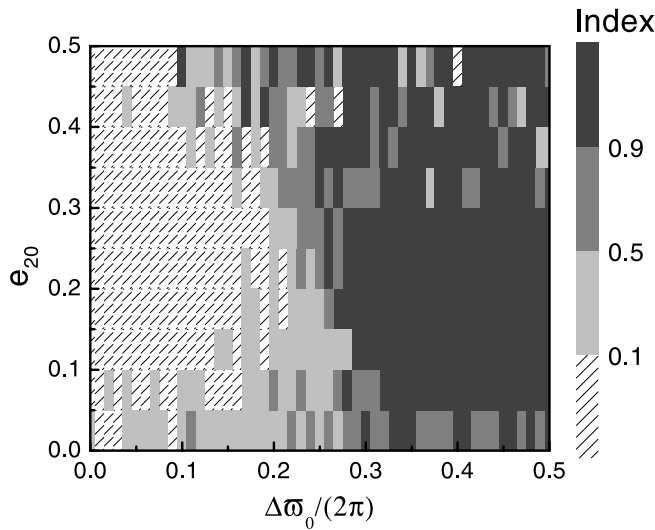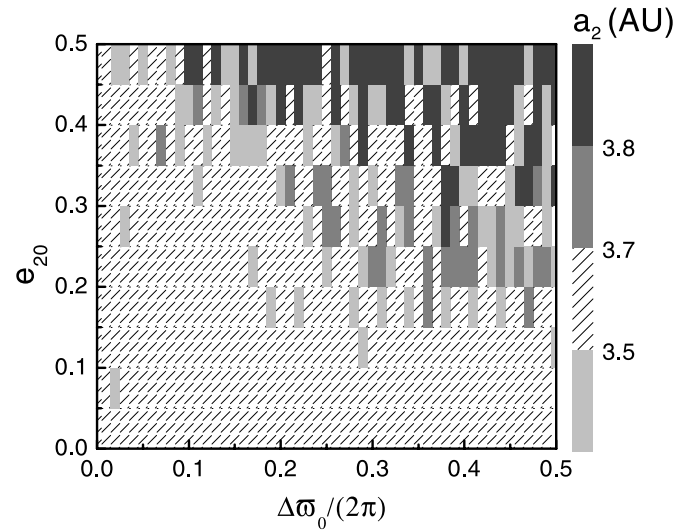
FIG. 11.—(*a*) Index of libration region and (*b*) the relative semimajor axis of two planets HD 12661 systems under azimuthal acceleration $f_2 = -2 \times 10^{-6}$ AU^2 yr^{-1}. The initial eccentricity is $e_{10} = 0.35$ and M_{10}, M_{20} are randomly chosen. The evolution time is $t = -50,000$ yr.

configurations of apsidal resonance are generally preserved during the migration. Thus, most of planet systems that are observed in apsidal resonance now might be in resonance before the migration begins. Again, the orbits in aligned resonance seem to be more stable in the sense of having modest final a_2, which may be the result of fewer close encounters between the two planets.

4. CONCLUSIONS AND DISCUSSIONS

In this paper, we have studied the occurrence as well as the stability of the apsidal resonance. The apsidal resonance occurs when the equations (19) and (20) are fulfilled. We find the occurrence of apsidal resonance depends only on the mass ratio $q = m_1/m_2$, the semimajor axis ratio $\alpha = a_1/a_2$ (in secular systems, a_1, a_2 are constants), initial eccentricity ratio e_{10}/e_{20}, and the relative apsidal longitude $\varpi_{20} - \varpi_{10}$ of the two planets. The criteria are based on the Laplace-Lagrange secular solution of linear perturbation theory. Based on these criteria, the ratio of librating to nonlibrating orbits in the e_{20}-$\Delta\varpi_0$ plane can be obtained analytically, which is given in equations (23) and (26). We also find for two planets on the orbits with large eccentricities that they can be in a stable configuration only when they are in aligned apsidal resonance. When the planets are migrated under the planet-disk interactions, more than half of the studied orbits preserves the configurations of apsidal resonance.

The linear secular perturbation theory is applicable only when the two planets are not in a lower order mean motion resonance. In lower order resonances, the variations of ϖ_1 and ϖ_2 are not guided by the secular dynamics, but by the resonance angles. For example, for the $j : (k - j)$ resonance, if the two resonance angles $\theta_1 = j\lambda_1 + (k - j)\lambda - k\varpi_1$, $\theta_2 = j\lambda_1 + (k - j)\lambda - k\varpi_2$ librate around 0 or π, then the relative longitude of pericenter $\Delta\varpi = (\theta_1 - \theta_2)/k$ must librate around either 0 or π. Thus, we think in this case, the lower order mean motion resonance and the apsidal resonance are not independent, and the former guides the dynamics. In the case that only θ_1 librates, we believe that the apsidal resonance is very unlikely to occur, since in this

case ϖ_1 is guided by θ_1; thus, it cannot have variations similar to ϖ_2.

Beaugé, Ferraz-Mello, & Michtchenko (2002) find that there may exist some asymmetric stationary solutions in the mean motion resonance region, where both the resonant angles and $\Delta\varpi$ are constants with values different from 0 or π. We think such kinds of solutions are due to the mean motion resonance and can exist only in the resonance regions, since such kinds of apsidal resonance solutions with $\Delta\varpi$ librating about constants with values different from 0 or π cannot be found in the linear secular perturbation system.

For the 10 known multiple-planet systems (see Table 8 of Fischer et al. 2003 for a list of the elements), the situation of whether apsidal resonance happens between their planets can be classified roughly into three groups (see Table 3 for the extensions of $\Delta\varpi_0$ when apsidal resonance would occur for the observed q, α, e_{20}/e_{10}):

(1) *Planets both in apsidal resonance and mean motion resonance.*—55 Cancri b and c (Fig. 12*a*), GJ876 b and c, and HD 82943 b and c are in apsidal resonance, since they are at the mean resonances 3 : 1, 2 : 1, and 2 : 1, respectively. In fact, HD 82943 b and c can be in apsidal resonances without in the mean motion resonance, while GJ876 b and c are near the boundary of libration according to the linear secular dynamics (Fig. 13*a*).

(2) *Planets in apsidal resonances far away from lower order mean motion resonances.*—HD 12661 b and c, 47 UMa b and c, and υ And c and d (Fig. 12*b*) are in this type. They are in apsidal resonance without the existence of any strong mean resonances. Moreover, HD 12661 b and c seem to be in antialigned apsidal resonance, which is within the boundary of a chaotic region.

(3) *Planets not in apsidal resonance either because of the negligible small libration region in the e_{20}-$\Delta\varpi_0$ plane or without suitable $\Delta\varpi_0$.*—The two planets in HD 38529, HD 168443, and HD 74156 are not in apsidal resonance, since the libration regions in the e_{20}-$\Delta\varpi_0$ plane are negligibly small for the observed q, α, and e_2/e_1 (Table 3). HD 37124 b and c have a large aligned libration area for the present parameters, and their eccentricities are not small,

TABLE 3

EXTENSIONS OF $\Delta\varpi_0$ IN APSIDAL RESONANCE FOR THE OBSERVED SYSTEMS

Planet Pair	$q = m_1/m_2$	$\alpha = a_1/a_2$	e_{10}/e_{20}	Aligned $\Delta\varpi_0$ (deg)	Antialigned $\Delta\varpi_0$ (deg)
υ And b–c....................	0.358	0.0720	0.037	$(-79.3, 79.3)$	...[a]
υ And b–d	0.181	0.0228	0.040	$(-47.0, 47.0)$	...
υ And c–d....................	0.507	0.317	1.08	$(-9.0, 9.0)$	...
55 Cnc b–c....................	4.15	0.477	0.073	...	$(96.8, 263.2)$
55 Cnc b–d	0.225	0.021	0.107	...	...
55 Cnc c–d....................	0.054	0.044	1.46	...	...
GJ876 c–b	0.296	0.628	2.70	...	$(144.0, 216.0)$
47 UMa[b] b–c	3.34	0.560	12.2	$(-87.9, 87.9)$	...
HD 37124 b–c	0.860	0.184	0.250	$(-69.8, 69.8)$	...
HD 12661 b–c	1.46	0.320	1.75	$(-67.8, 67.8)$	$(98.6, 261.4)$
HD 82943 c–b	0.540	0.628	1.32	$(-59.7, 59.7)$	$(132.8, 227.2)$
HD 168443 b–c	0.450	0.103	2.65	...	...
HD 38529 b–c	0.061	0.035	0.806	...	...
HD 74156[c] b–c	0.208	0.080	1.625	...	...

[a] Here ellipses mean no possible libration $\Delta\varpi_0$.
[b] Data from Fischer et al. 2002.
[c] Data from California and Carnegie Planet Search (see footnote 1).

but they are not in resonance because of the present values of $\Delta\varpi_0$ if $\Omega_b = \Omega_c = 0$ is assumed (Fig. 13b).

However, because of the unknown of the inclinations and the longitude of ascending nodes in the orbital fit from the observation data, it is still too early to make conclusions for some planet systems as to whether the planets are in apsidal resonances. For example, HD 12661 b and c are believed to be in the antialigned libration now. This is achieved by assuming $\Omega_1 = \Omega_2 = 0$, and they are on the boundary of a chaotic region. Alternative choices of Ω_i ($i = 1, 2$) might change the conclusion. Especially if we chose $\Omega_1 - \Omega_2 \sim 180°$, the two planets will be in the aligned apsidal resonance, which is stable according to Figure 9b. Similarly, HD 37124 b and c could be in apsidal resonance if suitable parameters Ω are observed.

Similar secular resonance might also happen because of nearly the same averaging precessing rate of the ascending nodes between the two planets in mutually inclined orbits. Since the inclination perturbations are isolated from the eccentricity ones in linear secular perturbation theory, we address this problem in a separate paper (Zhou & Sun 2004, in preparation).
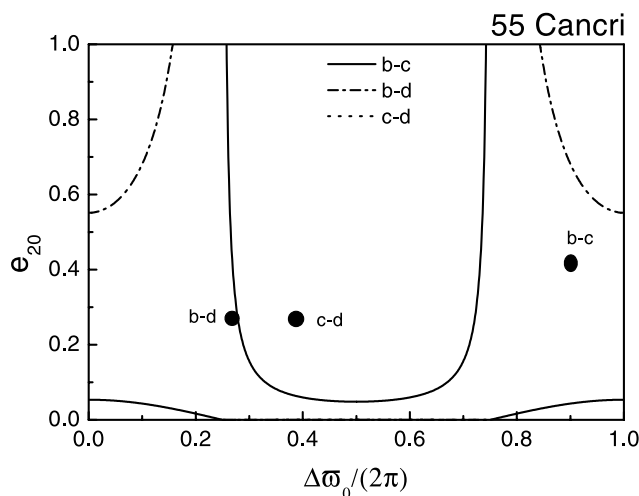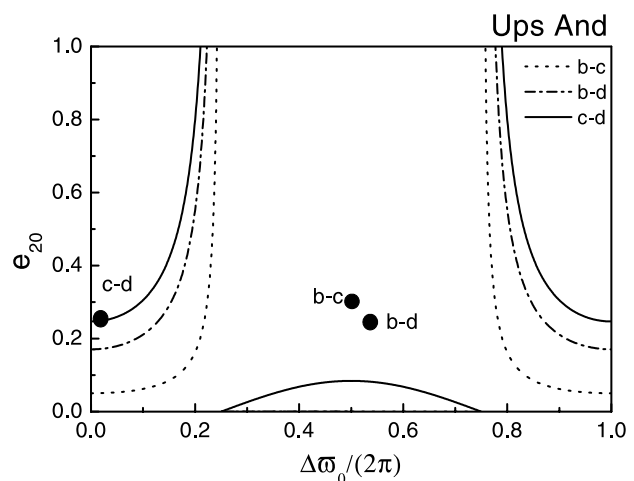
FIG. 12a

FIG. 12b

FIG. 12.—Libration region in the initial e_{20}-$\Delta\varpi_0$ plane defined by eqs. (19) and (20) for the two triple-planet systems (a) 55 Cancri ($\varpi_b = 99°, \varpi_c = 61°$, and $\varpi_d = 201°$); (b) υ Andromedae ($\varpi_b = 73°, \varpi_c = 250°$, and $\varpi_d = 260°$). Invisible boundary curves are out of the range of e_{20}. The filled circles show the present configuration of the two planets. Other orbital elements are taken from Fischer et al. (2003).
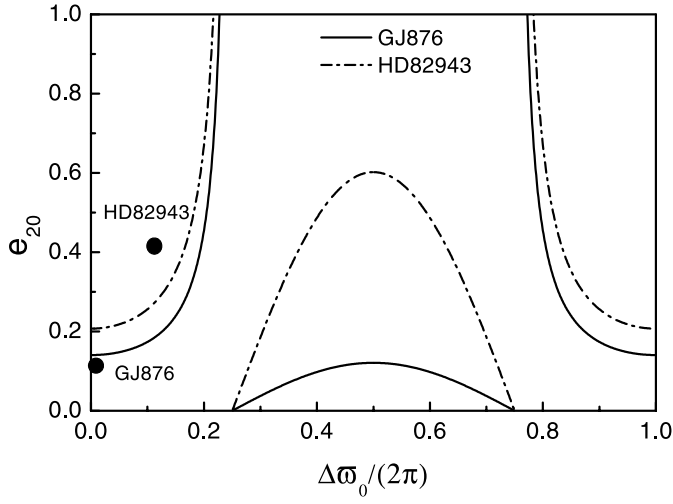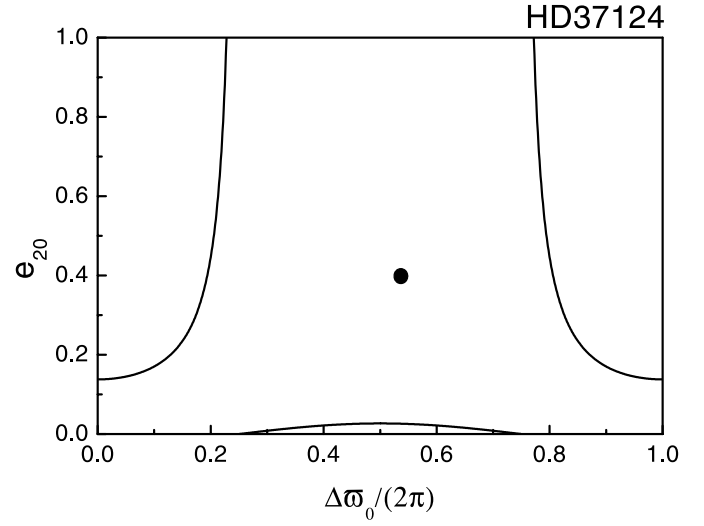
FIG. 13a

FIG. 13b

FIG. 13.—Libration region in the initial e_{20}-$\Delta\varpi_0$ plane defined by eqs. (19) and (20) for the planetary system (a) GJ876 ($\varpi_b = 330°$, $\varpi_c = 333°$), HD 82943 ($\varpi_b = 96°$, $\varpi_c = 138°$); (b) HD 37124 ($\varpi_b = 60°$, $\varpi_c = 259°$). The filled circles show the present configuration of the two planets. Other orbital elements are taken from Fischer et al. (2003).

REFERENCES

Beaugé, C., Ferraz-Mello, S., & Michtchenko, T. A. 2003, ApJ, 593, 1124
Chiang, E. I., Tabachnik, S., & Tremaine, S. 2001, AJ, 122, 1607
Fischer, D. A., Marcy, G. W., Butler, R. P., Laughlin, G., & Vogt, S. S. 2002, ApJ, 564, 1028
Fischer, D. A., Marcy, G. W., Butler, R. P., Vogt, S. S., Henry, G. W., Pourbaix, D., Walp, B., Misch, A. A., & Wright, J. T. 2003, ApJ, 586, 1394
Goździewski, K., & Maciejewski, A. J. 2001, ApJ, 563, L81
———. 2003, ApJ, 586, L153

Ji, J. H., Kinoshita, H., Liu, L., & Li, G. Y. 2003, ApJ, 585, L139
Kiseleva-Eggleton, L., Bois, R., Rambaux, N., & Dvorak, R. 2002, ApJ, 578, L145
Laughlin, G., Chambers, J., & Fischer, D. 2002, ApJ, 579, 455
Lee, M. H., & Peale, S. J. 2002, ApJ, 567, 596
———. 2003, ApJ, 592, 1201 (erratum, 597, 644)
Malhotra, R. 2002, ApJ, 575, L33
Murray, C. D., & Dermott, S. F. 1999, Solar System Dynamics (Cambridge: Cambridge Univ. Press), 274
Ward, W. R. 1997, Icarus, 126, 261